Proceedings of the 21st International Conference on Low Temperature Physics
Prague, August 8–14, 1996

Part S6 – Plenary and invited papers

Spin and orbital orderings and their excitations in perovskite Mn oxides

J. Inoue[a], S. Ishihara[b], W. Koshibae[c], Y. Kawamura[a], S. Okamoto[a] and S. Maekawa[a,d]

[a] Department Applied Physics, Nagoya University, Nagoya 464-01 Japan

[b] Department of Applied Physics, University of Tokyo, Tokyo 113, Japan

[c] CIRSE, Nagoya University, Nagoya 464-01, Japan

[d] Institute for Materials Research, Tohoku University, Sendai 980-77 Japan

An effective Hamiltonian, which includes a coupling between spins and orbitals, is derived for manganites by taking into account the Hund coupling, on-site Coulomb interaction and orbital degeneracy of the e_g state. By using the effective Hamiltonian, magnetic structures, spin and orbital excitations are studied in a mean field approximation for the undoped insulating phase and in the exact diagonalization method for the undoped and 50 % doped charge-ordered phases. It is shown that the coupling between spins and orbitals is crucial to the magnetic structures and that the so-called A-type AF is realized by self-adjusting the orbital ordering. Implication to the colossal magnetoresistance in manganites is given.

1. INTRODUCTION

Recently, a huge negative magnetoresistance called colossal magnetoresistance (CMR) has been observed in perovskite manganites (La-X)MnO_3 where X is Ba, Ca, or Sr [1, 2, 3, 4, 5, 6]. The phase diagram of the manganites shows a rich variety of structural, magnetic, and transport properties [7, 8, 9, 10]. The undoped manganite, $LaMnO_3$, is an insulator with a layered antiferromagnetism (AF), A-type AF, and changes to a ferromagnetic (F) metal by replacing La with Ba, Ca or Sr. A complex spin and charge ordered phase, CE-type AF, occurs near 50% doping of Ca. In the Ca rich region, the stripe type AF (C-type AF) appears, and finally the usual alternate type AF (G-type AF) occurs in $CaMnO_3$. Near the Curie temperature in F state, the resistivity dramatically drops with decreasing temperature, and the CMR appears by relatively weak external magnetic fields. The CMR effect is more dramatic in $La_{0.5}Ca_{0.5}MnO_3$, $Pr_{0.5}Sr_{0.5}MnO_3$, and $Pr_{0.5}Ca_{0.5}MnO_3$, where the charge ordered AF insulating phase changes to the metallic F [11, 12]. This is actually an insulator-metal transition. The transition driven by relatively weak magnetic fields suggests that magnetically ordered phases are nearly degenerate. Therefore, the mechanism of appearance of these ordered phases is crucial to clarify the origin of CMR effect.

The magnetic and magnetotransport properties are governed by mainly Mn ions and less affected by oxygen ions. In $LaMnO_3$, Mn ions are Mn^{3+} and they become mixed-valent states of Mn^{3+} and Mn^{4+} in (La-X)MnO_3. The $3d$-electronic states of Mn ions split to doubly degenerate e_g states and triply degenerate t_{2g} states because of the crystal field from the cubic octahedron. As Mn^{3+} ions have $3d^4$ configuration, the t_{2g} states are occupied by three electrons with parallel spins and one e_g orbital is occupied by the remaining electron whose spin is parallel to t_{2g} spins due to the Hund coupling. $LaMnO_3$ is an insulator because of the strong on-site Coulomb interaction between e_g electrons and becomes metallic in the mixed-valent state where some Mn ions have no e_g electrons. The t_{2g} electrons behave as localized spins because the overlap of the wave functions between the t_{2g} and oxygen p orbitals is very small.

Thus, the key to understand the properties of manganites may reside on following ingredients of Mn ions; (1) Hund coupling between t_{2g} and e_g electron spins, (2) degeneracy of e_g states, and (3) on-site Coulomb interaction between e_g electrons. The first plays an important role in the double exchange (DE) interaction when mobile carriers is introduced. The phenomenon that the insulating A-type AF is changed to a metallic F state by doping has been understood in terms of the DE interaction [13]. The de-

generacy of e_g states causes the Jahn-Teller (JT) distortion, which has been suggested to be an origin of the insulating A-type AF in $LaMnO_3$ [14, 15]. Both the DE and JT mechanisms have been proposed to explain the CMR effect [16, 17, 18]. In these theories, however, the on-site Coulomb interaction between e_g electrons has been neglected though it is stronger in magnitude than the Hund coupling and the JT splitting of the e_g states [19]. We have previously shown that the strong on-site Coulomb interaction modifies the results obtained in the simple DE interaction and is important also for the magneto-transport [20]. The on-site Coulomb interaction has also been pointed out to give rise to a coupling between spin and orbital degrees of freedom in combination with the orbital degeneracy [21, 23, 22, 24, 25].

In this paper, we will show that the coupling between spins and orbitals actually plays a crucial role on the magnetic structures and excitations in manganites. In the following, we first derive an effective Hamiltonian for manganites by taking into account the key ingredients mentioned above. Using the effective Hamiltonian, we study spin and orbital orderings and their excitations for undoped insulating phase in a mean field approximation [26]. Next, an interplay of the spins and orbitals is demonstrated in the exact diagonalization (ED) study for both undoped insulating phase and the charge ordered phase with 50% doping [27]. Finally, we briefly discuss implications to the CMR effect.

2. EFFECTIVE HAMILTONIAN

The basic Hamiltonian consists of hopping of e_g electrons between nearest neighbor (n.n.) Mn ions, the Hund coupling between itinerant e_g and localized t_{2g} spins, on-site Coulomb interaction between e_g electrons, and AF coupling between n.n. localized t_{2g} spins. The hopping matrix elements between $d_{x^2-y^2}$ and $d_{3z^2-r^2}$ orbitals are properly evaluated in the tight-binding model including oxygen p-orbitals and the last term is included to realize the G-type AF of $CaMnO_3$.

Eliminating the on-site Coulomb interaction, which has the largest energy scale, in the usual second-order perturbation method excluding the double occupancy of the e_g orbitals, we obtain the effective Hamiltonian, which includes the coupling between spin and orbital degrees of freedom [26]. The final expression of the effective Hamiltonian is given by

$$H_{eff} = H_0 + \tilde{H}_{e_g} + H_K + H_{Jt_{2g}}, \qquad (1)$$

with

$$H_0 = \sum_{i\sigma\mu} \epsilon_d \tilde{c}^\dagger_{i\mu\sigma}\tilde{c}_{i\mu\sigma} + \sum_{ij\sigma\mu\nu} t^{\mu\nu}_{ij}\tilde{c}^\dagger_{i\mu\sigma}\tilde{c}_{j\nu\sigma}, \qquad (2)$$

$$\begin{aligned}\tilde{H}_{e_g} = & -2\tilde{J}\sum_{<ij>}\left(\frac{3}{4}n_i n_j + \mathbf{S}_i\cdot\mathbf{S}_j\right) \\ & \times \left[\left(t^{aa2}_{ij}+t^{bb2}_{ij}\right)\left(\frac{1}{4}n_i n_j - T^z_i T^z_j\right)\right. \\ & + \left(t^{ab2}_{ij}+t^{ba2}_{ij}\right)\left(\frac{1}{4}n_i n_j + T^z_i T^z_j\right) \\ & - t^{aa}_{ij}t^{bb}_{ij}\left(T^+_i T^-_j + T^-_i T^+_j\right) \\ & - t^{ab}_{ij}t^{ba}_{ij}\left(T^+_i T^+_j + T^-_i T^-_j\right) \\ & - \left(t^{ba}_{ij}t^{aa}_{ij} - t^{ab}_{ij}t^{bb}_{ij}\right)\left(T^+_i T^z_j + T^-_i T^z_j\right) \\ & \left. - \left(t^{ab}_{ij}t^{aa}_{ij} - t^{ba}_{ij}t^{bb}_{ij}\right)\left(T^z_i T^+_j + T^z_i T^-_j\right)\right] \qquad (3)\end{aligned}$$

$$H_K = -\frac{K}{2}\sum_{i\mu\sigma_1\sigma_2}\mathbf{S}^{t_{2g}}_i\cdot c^\dagger_{i\mu\sigma_1}\boldsymbol{\sigma}_{\sigma_1\sigma_2}c_{i\mu\sigma_2}, \qquad (4)$$

$$H_{Jt_{2g}} = J_{t_{2g}}\sum_{<ij>}\mathbf{S}^{t_{2g}}_i\cdot\mathbf{S}^{t_{2g}}_j. \qquad (5)$$

Here, H_0 stands for the hopping of e_g electrons from an orbital μ on site i to an orbital ν on the n.n. site j with a constraint that no double occupancy of the e_g state permitted. $\tilde{H}_{e_g}$ is the super-exchange type effective Hamiltonian for e_g electrons, which is expressed in terms of the spin operator $\mathbf{S}$ and pseudospin operator $\mathbf{T}$ of e_g electrons, which are defined by

$$\mathbf{S}_i = \frac{1}{2}\sum_{\mu,\alpha,\beta}\tilde{c}^\dagger_{i\mu\alpha}\boldsymbol{\sigma}_{\alpha\beta}\tilde{c}_{i\mu\beta} \qquad (6)$$

and

$$\mathbf{T}_i = \frac{1}{2}\sum_{\alpha,\mu,\nu}\tilde{c}^\dagger_{i\mu\alpha}\boldsymbol{\sigma}_{\mu\nu}\tilde{c}_{i\nu\alpha}, \qquad (7)$$

respectively, where $\boldsymbol{\sigma}$ is the Pauli matrix. $\mathbf{T}$ denotes the orbital degree of freedom of the e_g electrons. The eigenstates of the operator $\mathbf{T}$ correspond to the occupied and unoccupied e_g orbitals, for example, $T_z = 1/2$ and $-1/2$ correspond to the occupied $d_{x^2-y^2}$ and $d_{3z^2-r^2}$, respectively. In $\tilde{H}_{e_g}$, $\tilde{J} = t_0^2/(U'-J')$ with inter-orbital Coulomb interaction U', inter-orbital exchange interaction J' within the same ion, and a hopping integral t_0 between two neighboring $d_{x^2-y^2}$ orbitals in the x direction. t^{ab}_{ij} is a hopping integral between a and b orbitals normalized by t_0. H_K and $H_{t_{2g}}$ denote the Hund coupling between e_g electrons and localized t_{2g} spins, $\mathbf{S}^{t_{2g}}$, and AF interaction between localized t_{2g} spins, respectively. Other notations are standard. In $\tilde{H}_{e_g}$,

we have omitted two terms whose prefactors include K in the denominator thereby their contribution is small. The three-site hopping term was also neglected as usually done in the transformation from the Hubbard model to the $t-J$ model [26].

We can see from the expression of $\tilde{H}_{e_g}$ that the coupling constant depends on the hopping integrals between n.n. sites, thereby it depends on the type of orbital ordering. Basically, $\tilde{H}_{e_g}$ prefers F ordering in the spin part and AF ordering in the orbital part. However, the orbital ordering is not so simple as described above because of complex terms like $T_i^{\pm}T_j^{\pm}$. Because the Hund coupling is usually strong in manganites, the F spin coupling in $\tilde{H}_{e_g}$ competes with the AF coupling between the t_{2g} spins. Therefore, determination of the magnetic structure is highly nontrivial because the coupling constant in $\tilde{H}_{e_g}$ depends on orbital ordering. In the following we show that various magnetic orderings appear near the realistic parameter values.

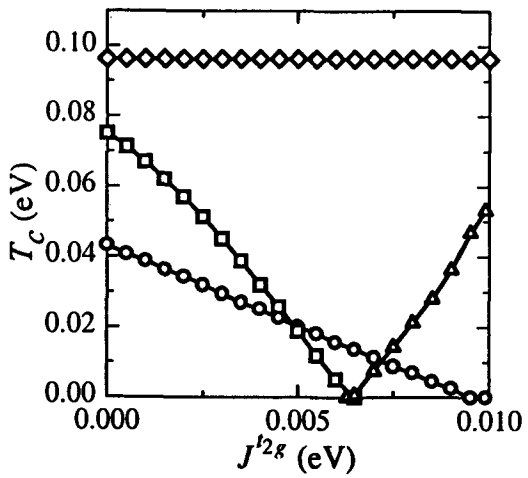

Figure 1: Transition temperatures as functions of $J_{t_{2g}}$ for F (squares), A-type AF (circles), G-type AF (triangles) and for orbital ordering (diamonds).

3. CALCULATED RESULTS

3.1. Mean field approximation

In this section, we present the results of the transition temperature T_C of spin and orbital orderings and the excitations calculated for the insulating $LaMnO_3$ in a mean field approximation. Throughout this section, we take $\tilde{J} \sim 0.1$ eV and assume $[3x^2-r^2, 3y^2-r^2]$ type orbital ordering [28] where $d_{3x^2-r^2}$ and $d_{3y^2-r^2}$ orbitals are occupied alternately by one e_g electron. In the calculation, we have included two terms which are not explicitly shown in the expression of $\tilde{H}_{e_g}$. These terms effectively increase the AF coupling between e_g spins.

Fig. 1 shows the calculated results of T_C as functions of $J_{t_{2g}}$. We have introduced the following thermal averages, $\langle S_z\rangle, \langle T_z\rangle, \langle S_zT_z\rangle$ and $\langle S_z^{t_{2g}}\rangle$ as the mean fields. We can see in the figure that the highest T_C of the spin ordering changes in order of F, A-type AF and G-type AF with increasing $J_{t_{2g}}$. The A-type AF is realized for intermediate values of $J_{t_{2g}}$ near 6 meV with $T_C = 0.015 \sim 0.02$ eV. The value of $J_{t_{2g}}$ to realize the A-type AF is the same order of magnitude with that estimated from the Néel temperature T_N of $CaMnO_3$. T_C for the A-type AF is also consistent with $T_N \sim 140$ K in $LaMnO_3$.

T_C of the $[3x^2-r^2, 3y^2-r^2]$ type orbital ordering is independent of $J_{t_{2g}}$ as expected and much higher than that of the spin ordering. The orbital ordering in the actual compounds may occur at the structural transition temperature (875 K) [9] from the rhombohedral to O'-orthorhombic phases. The calculated orbital ordering temperature is of the same order with the structural phase transition temperature.

The change in the spin structures with increasing $J_{t_{2g}}$ is brought about by a competition between the isotropic AF coupling between t_{2g} spins and the anisotropic F coupling in $\tilde{H}_{e_g}$. In the $[3x^2-r^2, 3y^2-r^2]$ type orbital ordering, magnitude of the electron transfer between the occupied $d_{3x^2-r^2}(d_{3y^2-r^2})$ orbital and its n.n. unoccupied $d_{3y^2-r^2}(d_{3x^2-r^2})$ orbital in the $x-y$ plane becomes much larger than that along z axis. Therefore, the F coupling in $\tilde{H}_{e_g}$ becomes anisotropic. The anisotropy is realized by including the inter-orbital transfer integrals. Actually, if we take $t_{ij}^{ab} = t_{ij}^{ba} = 0$, the A-type AF ordering can not be stabilized for any parameter values. Thus, the A-type spin ordering is a result of a competition between the AF interaction and the effective F coupling which is assisted by the orbital ordering.

Next, we examine the spin and orbital excitations in the A-type AF associated with the $[3x^2-r^2, 3y^2-r^2]$ type orbital ordering. In the calculations, we adopt an extended unit cell which contains four Mn ions and introduce a new spin operator **J** with $J=2$, replacing the spin operators **S** and $\mathbf{S}^{t_{2g}}$ with **J**/4 and (3/4)**J**, respectively, and eliminate H_K because the large Hund coupling makes e_g and t_{2g} spins precess in phase in the low energy states. The spin and orbital excitations have been calculated by the Holstein-Primakoff transformation to both **J** and **T** operators and by the Hartree approximation.

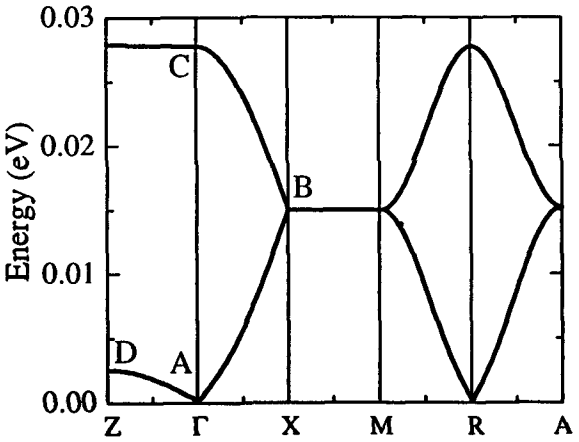

Figure 2: Spin wave excitation spectrum in the A-type AF ordering with $[3x^2-r^2, 3y^2-r^2]$ type orbital ordering.

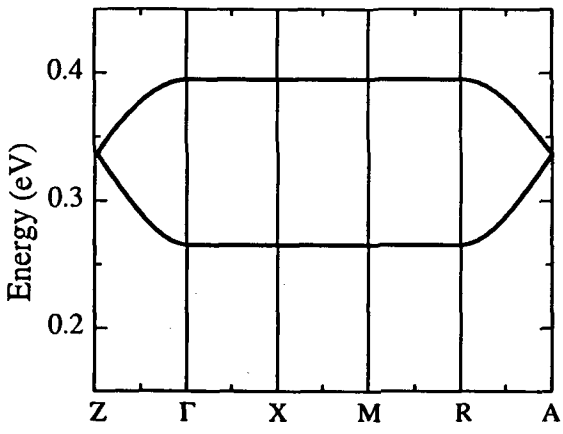

Figure 3: Orbital wave excitation spectrum in the A-type AF ordering with $[3x^2 - r^2, 3y^2 - r^2]$ type orbital ordering.

Results of the spin excitations are shown in Fig. 2 with $J_{t_{2g}} = 5.5$ meV. Other parameter values are the same with those used before. The dispersion curves along $A \rightarrow B \rightarrow C$ corresponds to those in $(0,0,0) \rightarrow (\pi/a, \pi/a, 0)$ in the Brillouin zone for the unit cell of the conventional perovskite structure with a being the lattice constant. The curve along $A \rightarrow D$ corresponds to that in $(0,0,0) \rightarrow (0,0,\pi/a)$ direction. The excitation energy in $(0,0,0) \rightarrow (\pi/a, \pi/a, 0)$ direction is much larger than that in $(0,0,0) \rightarrow (0,0,\pi/a)$ direction, indicating the two-dimensional character in the spin ordering. The calculated results in Fig. 2 show a good agreement with recent neutron measurements [29].

The calculated results of the dispersion of the orbital wave are shown in Fig. 3. There is a large energy gap in the orbital excitations, which may be resulted from an anisotropy introduced by the assumption of the layered type spin ordering, that is, the A-type AF in the ground state. Because there is no competition between the F and AF coupling as in the spin space, the orbital exications have a much wider band width as compared with the spin wave excitations. The flat dispersion in the $x-y$ plane is due to the $[3x^2 - r^2, 3y^2 - r^2]$ type of the orbital ordering, where the coefficients $t_{ij}^{aa}t_{ij}^{bb}$ and $t_{ij}^{ab}t_{ij}^{ba}$ in $\tilde{H}_{e_g}$ become zero.

3.2. Exact diagonalization method

In the mean field approximation, the type of the orbital ordering is assumed to be the observed one, $[3x^2-r^2, 3y^2-r^2]$ type orbital ordering. The spin and orbital ordering, however, must be determined self-consistently. In order to confirm the results obtain in the mean field approximation, we perform an exact diagonalization study for small clusters ($2 \times 2 \times 2$ in this case) using a simpler but effectively the same Hamiltonian for the insulating phase of $LaMnO_3$. Furthermore, we present the results calculated for a charge ordered phase with 50 % doping. In this section, we will show that the orbitals play an important role on the stabilization of the magnetic structures.

As we have reported in the previous section, the magnetic structures in the insulating phase of $LaMnO_3$ are realized by a competition between the AF coupling between t_{2g} spins and an effective F coupling in $\tilde{H}_{e_g}$ where the type of the orbital ordering governs the coupling constant. Because the Hund coupling is strong enough to make e_g and t_{2g} spins parallel, we can introduce a supplementary isotropic AF interaction between e_g spins instead of H_K and $H_{Jt_{2g}}$ to represent the competing interactions between the AF coupling in $H_{Jt_{2g}}$ and the F coupling in $\tilde{H}_{e_g}$. The resultant Hamiltonian for the insulating phase may be written as

$$H = \tilde{H}_{e_g} + J_{AF} \sum_{<ij>} \mathbf{S}_i \cdot \mathbf{S}_j, \qquad (8)$$

which is characterized by two parameters $\tilde{J}$ and J_{AF}. This Hamiltonian may be sufficient to describe the low energy excitations. It should be noted that the magnitude of J_{AF} is larger than $J_{t_{2g}}$ by one order of magnitude because $\mathbf{S}^{t_{2g}}$ has been replaced with e_g spin S. With this simplification, we can treat three-

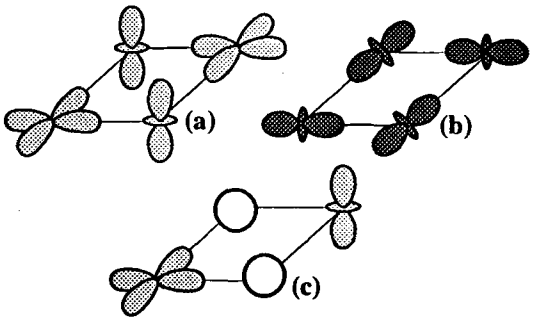

Figure 4: Types of orbital orderings; (a) F, C- and G-type AF in the undoped phase, (b) A-type AF in the undoped phase, and (c) A-type AF in the 50 % doped charge-ordered phase.

dimensional (3-D) 8-site ($2\times2\times2$) clusters in the ED method. One should note that the proper symmetry of the system is retained only when the 3-D is taken into account.

By examining the total spin value S^{tot} and spin correlation function $S(\mathbf{Q})$, it has been found that the spin ordering changes in order of F, A-type AF, C-type AF and G-type AF with increasing $J_{AF}/\tilde{J}$. The A-type AF is stabilized near $J_{AF}/\tilde{J} \sim 1.0$. Type of the orbital ordering can be identified by calculating the orbital correlations $\langle \mathbf{T}_i \cdot \mathbf{T}_j \rangle$. The orbital ordering in F, C and G-type AF is $[x^2-y^2, 3z^2-r^2]$ type, which is shown in Fig. 4(a). In the $[x^2-y^2, 3z^2-r^2]$ type ordering, the F coupling along the z-axis is stronger than that within the $x-y$ plane. Therefore, the F ordering naturally changes to C- and G-type AF with increasing $J_{AF}/\tilde{J}$. In this orbital ordering, however, the A-type AF does not appear. The A-type AF occurs only when the orbital ordering is rearranged to $[3x^2-r^2, 3y^2-r^2]$ type ordering, which is shown in Fig. 4(b). In this orbital ordering the F coupling along the z-axis is weaker than that in the $x-y$ plane. Therefore, the orbitals adjust themselves to lower the GS energy by realizing four F bonds and two AF bonds in the A-type AF for small values of $J_{AF}/\tilde{J}$. In the previous section, the $[3x^2-r^2, 3y^2-r^2]$ type orbital ordering has been assumed and the occurence of the A-type AF has been explained in the mean field approximation. In ED method, however, the stabilization of the A-type AF is self-consistently determined as a result of the strong interplay of spins and orbitals. Thus, the results confirm those obtained in the previous section. It should be stressed here that the A-type AF is realized by the strong on-site Coulomb interaction and the orbital degeneracy.

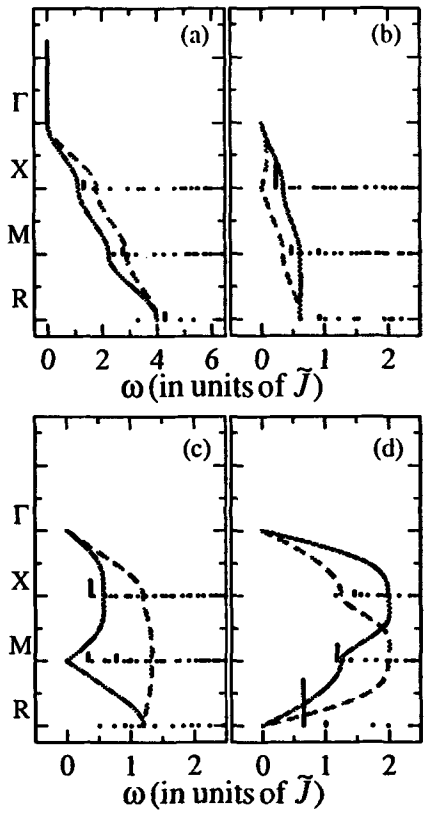

Figure 5: Numerical results of the spin excitation spectra of (a) F, (b) A-type AF, (c) C-type AF and (d) G-type AF in the insulating phase for a $2\times2\times2$ cluster. The solid and broken curves are excitations in the $x-y$ plane and along z-axis,respectively, calculated in the spin wave approximation. Γ, X, M and R denote $\mathbf{Q} = (0,0,0), (\pi,0,0), (\pi,\pi,0)$ and (π,π,π), respectively.

We have studied the spin excitations in F, A-, C- and G-type AF in the ED method and compared the results with those in the spin wave approximation. The results are shown in Fig. 5, where the solid and broken lines are calculated ones by the spin wave approximation with the same parameter values used in the ED method. We found that the spectra with strong intensity appear approximately in the region where the spectra in the spin wave approximation ex-

ist, and that incoherent spectra with weak intensity spread over high frequency region. The incoherent part is caused by the coupled excitations of spins and orbitals. In spite of the coupling, the main feature of the low-energy spectra can be qualitatively explained in the spin wave approximation, which may justify the usual spin wave analysis presented in the previous section for the experimental results in $LaMnO_3$ [29]. The orbital excitations are rather difficult to analyze because the total angular momentum does not conserve as can be seen in the Hamiltonian, so we omit detailed discussion of the orbital excitations.

The charge ordered state at 50% doping shows a complex ordering of the CE-type AF. As the size of the unit cell, containing 16 Mn atoms in the CE-type AF, is too large for the ED method, we focus our attention on how the interplay of spins and orbitals can be realized in a NaCl-type charge ordering. This problem is highly nontrivial because the hopping of e_g electrons to a n.n. vacant site leads to a gain in the kinetic energy and produces additional interactions. The important point is that the kinetic energy depends on the orbital orderings.

In order to realize the charge ordered phase, we add a term of n.n. Coulomb repulsion, $\sum_{<ij>} V n_i n_j$. As the e_g electrons are mobile, the simplification used for the undoped case can not be allowed and the t_{2g} and e_g spins must be dealt with separately. In the following, we take relatively large values of K and V to ensure the parallel alignment of e_g and t_{2g} spins on the same site and the charge ordering. Now the competing interactions are the AF interaction between t_{2g} spins and the F couplings due to the effective Hamiltionian derived for e_g electrons and the DE type interaction caused by the hopping of e_g electrons. Here, we assume 1/2 spin for t_{2g} spins to make the ED calculation possible for $2 \times 2 \times 2$ dice. Parameter values are taken as $\tilde{J} = 0.1|t_0|$ and $V = K = 10|t_0|$.

The type of spin ordering calculated as a function of $J_{t_{2g}}/t_0$ changes in order of F, A-type AF, C-type AF and Ferri with increasing $J_{t_{2g}}/t_0$. However, the ground state is degenerate except for the A-type AF, calculation of $S(\mathbf{Q})$ is useless to identify the the C-type AF. Therefore, the stabilization of the C-type AF is not conclusive. The parameter range of the stabilization of AF is rather narrow, $0.01 < J_{t_{2g}}/t_0 < 0.04$. In the Ferri state, spins of Mn^{3+} and Mn^{4+} align alternately, and the S^{tot} becomes 2 for 8-site clusters. The types of the orbital ordering within the $x-y$ plane can be obtained from the orbital correlations $\langle \mathbf{T}_i \cdot \mathbf{T}_j \rangle$. They are shown in Fig. 4(c) for A-type AF ordering. We can interpret that the A-type AF is realized by adjusting the orbital ordering as in the undoped case. This is an interplay of spin and orbital degrees of freedom, which is crucial for the magnetic structures of manganites.

4. DISCUSSION

As shown in previous sections, there can be several types of AF ordering within narrow parameter regions. The variety of the magnetic ordering suggests that the CE-type AF can be realized in larger clusters than those used in the present calculations, and that the spin ordering of the GS can easily be changed by some external forces such as magnetic field and pressure [31, 32]. The effect of the magnetic field is nothing but the CMR effect, which is most remarkable in the charge ordered phase [12]. In usual magnets, the energy difference between F and AF states is so large that the magnetic state can not be easily changed by the external magnetic field. However, in the manganites, the interplay of spins and orbitals makes the variety of magnetic structures possible and leads to the large magnetoresistance effect.

The 50 % doped manganites show the CE-type AF which has complex magnetic ordering. The size of the clusters in our ED study is too small to realize this structure. However, in a preliminary calculation for a $\sqrt{8} \times \sqrt{8}$ cluster where the magnetic structure within the $a-b$ plane has been emphasized, the results of the spin correlations suggest that the magnetic structure is either a spiral state or a zigzag type AF ordering. The latter is the observed structure within the $a-b$ plane in the CE-type AF. The orbital correlations are also in accord with the observed CE-type structure [9, 30].

5. CONCLUSION

We have derived an effective Hamiltonian for manganites, which includes strong coupling between spin and orbital degrees of freedom and competing ferromagnetic and antiferromagnetic interactions. By making use of the effective Hamiltonian, the spin and orbital orderings have been studied in the mean field approximation and the exact diagonalization method. It has been shown that various magnetic structures can be realized within the relatively narrow range of parameter values and that the role of orbital degree of freedom is crucial to the spin ordering. Especially, the A-type AF is stabilized by self-adjusting the orbital ordering. The spin and orbital excitations have also been studied in the mean

field approximation as well as in the exact diagonalization method. The results in the ED method have justified those in the mean field approximation. The calculated spin wave excitations of the A-type AF are in good agreement with those in the neutron experiment. The spin and orbital excitations also couple with each other. We stress the importance of the interplay of spins and orbitals caused by the strong on-site Coulomb interaction and orbital degeneracy to elucidate the magnetic properties as well as the CMR effect. Study for the metallic phase is a remaining issue to be studied near future.

ACKNOWLEDGEMENTS

The work was supported by a Grant-in Aid for Scientific Research on Priority-Areas from Ministry of Education, Science and Culture of Japan, and New Energy and Industrial Technology Development Organization (NEDO). Computations have been performed in the Computer Centers of Institute of Molecular Science, Okazaki National Research Institute, Institute for Materials Research, Tohoku University, and Institute for Solid State Physics, University of Tokyo.

REFERENCES

[1] R. M. Kusters, J. Singleton, D. A. Keen, R. McGreevy and W. Hayes, Physica B **155** (1989) 362.

[2] R. von Helmolt, J. Wecker, B. Holzapfel, L. Schultz, and K. Samwer, Phys. Rev. Lett. **71** (1993) 2331.

[3] K. Chahara, T. Ohono, M. Kasai, Y. Kanke and Y. Kozono, Appl. Phys. Lett. **62** (1993) 780.

[4] S. Jin, T. H. Tiefel, M. McCormack, R. A. Ffastnacht, R. Ramesh and L. H. Chen, Science **264** (1994) 413.

[5] Y. Tokura, A. Urushibara, Y. Moritomo, T. Arima, A. Asamitsu, G. Kido and N. Furukawa, J. Phys. Soc. Jpn. **63** (1994) 3931.

[6] H. Y. Hwang, S.-W. Cheong, P. G. Radaelli, M. Marezio, and B. Batlogg, Phys. Rev. Lett. **75** (1995) 914.

[7] G. H. Jonker and H. van Santen, Physica **16** (1950) 337.

[8] E. O. Wollan and W. C. Koehler, Phys. Rev. **100** (1955) 545.

[9] J. B. Goodenough, Phys. Rev. **100** (1955) 564.

[10] P. Schiffer, A. P. Ramirez, W. Bao, and S.-W. Cheong, Phys. Rev. Lett. **75** (1995) 3336.

[11] Y. Tomioka, A. Asamitsu, Y. Moritomo, H. Kuwahara, and Y. Tokura, Phys. Rev. Lett. **74** (1995) 5108.

[12] Y. Tokura, Y. Tomioka, H. Kuwabara, A. Asamitsu, Y. Moritomo, and M. Kasai, Physica C **263** (1996) 544.

[13] C. Zener, Phys. Rev. **82** (1951) 403, P. W. Anderson and H. Hasegawa, Phys. Rev. **100**, (1955) 675, and P.-G. de Gennes, Phys. Rev. **118** (1960) 141.

[14] T. Mizokawa and A. Fujimori, Phys. Rev. B**51** (1995) 12880.

[15] I. Solovyev, N. Hamada, and K. Terakura, Phys. Rev. Lett. **76** (1996) 4825.

[16] N. Furukawa, J. Phys. Soc. Jpn, **63** (1994) 3214.

[17] A. J. Millis, P. B. Littlewood, and B. I. Shraiman, Phys. Rev. Lett. **74** (1995) 5144, and A. J. Millis, B. I. Shraiman and R. Mueller, Phys. Rev. Lett. **77** (1996) 175.

[18] H. Röder, J. Zang, and A. R. Bishop, Phys. Rev. Lett. **76** (1996) 1356.

[19] S. Saitoh, A. E. Bocquet, T. Mizokawa, H. Namatame, A. Fujimori, M. Abbate, Y. Takeda, and M. Takano, Phys. Rev. B **51** (1995) 13942.

[20] J. Inoue and S. Maekawa, Phys. Rev. Lett. **74**, (1995) 3407, Physica C **235-240** (1994) 2199, **263** 138.

[21] L. M. Roth, Phys. Rev. **149** (1966) 306.

[22] K. I. Kugel and D. I. Khomskii, JETP Lett. **15** (1972) 446.

[23] M. Cyrot and C. Lyon-Caen, J. de Physique **36** (1975) 253.

[24] S. Inagaki, J. Phys. Soc. Jpn., **39** (1975) 596.

[25] C. Castellani, C. R. Natoli and J. Ranninger, Phys. Rev. B **18** (1978) 4945, see also T. M. Rice, *Springer Series in Solid-State Sciences, Eds. A. Fujimori and Y. Tokura* **119** (1995) 221.

[26] S. Ishihara, J. Inoue and S. Maekawa, Physica C **263**, (1996) 130, and to be published.

[27] W. Koshibae, Y. Kawamura, S. Ishihara, S. Okamoto, J. Inoue and S. Maekawa, to be published.

[28] G. Matsumoto, J. Phys. Soc. Jpn. **29** (1970) 606.

[29] K. Hirota, N.Kaneko, A. Nishizawa, and Y. Endoh, to be published.

[30] C. H. Chen and S-W. Cheong, Phys. Rev. Lett. **76**, (1996) 4042.

[31] Y. Moritomo, A. Asamitsu, and Y. Tokura, Phys. Rev. B **51** (1995) 16491.

[32] Recently, A-type AF has been reported for $Pr_{0.5}Sr_{0.5}MnO_3$ by Yoshizawa, unpublished.